

Experimental determination of the inhomogeneous contribution to linewidth in Permalloy films using a time-resolved magneto-optic Kerr effect microprobe

M. L. Schneider,^{a)} Th. Gerrits, A. B. Kos, and T. J. Silva
National Institute of Standards and Technology, Boulder, Colorado 80305, USA

(Received 12 March 2007; accepted 6 July 2007; published online 12 September 2007)

We adapted a time-resolved magneto-optic microprobe for use with a pulsed inductive microwave magnetometer apparatus, to measure the magnetization dynamics of a thin Permalloy film at micrometer and millimeter length scales under exactly the same experimental conditions. The optical microprobe has a spatial resolution of $1\ \mu\text{m}$. We compare the data obtained over these different length scales to quantitatively determine the localized inhomogeneous contribution to magnetic damping. When measured directly with the magneto-optic technique, the inhomogeneous contributions are in agreement with the value $88 \pm 16\ \text{A/m}$ ($1.1 \pm 0.2\ \text{Oe}$) extrapolated from PIMM measurements of linewidth versus frequency. [DOI: [10.1063/1.2772563](https://doi.org/10.1063/1.2772563)]

I. INTRODUCTION

High speed magnetic data storage requires a better understanding of the high frequency response of magnetic materials. To this end, several techniques in addition to classic ferromagnetic resonance (FMR) are now being employed to measure the high frequency susceptibility of thin magnetic films.¹⁻⁷ The Landau-Lifshitz-Gilbert (LLG) damping parameter is often determined by measuring the slope of field-swept linewidth versus resonance frequency.¹ While the LLG theory predicts an intercept at the origin for such a measurement, it is commonly found that this is not the case. Generally, such a nonzero offset of the linear fitted intercept at zero frequency is ascribed to localized inhomogeneous field contributions within a thin film.¹

The size scale of nonuniformities can be used to determine the effect of inhomogeneities on linewidth.⁸ If the length scale is sufficiently large, then the inhomogeneities manifest as localized field fluctuations that result in spatially decoupled, nonuniform precessional dynamics, whereas closer spacing will lead to collective excitations that are not localized at the site of the inhomogeneity and are more consistent with the picture of two-magnon scattering; i.e., the inhomogeneities then act as defects that scatter energy from the uniform mode into nearly degenerate magnon modes. The critical characteristic length scale for this cross-over point from decoupled (inhomogeneous broadening) to collective excitations (two-magnon scattering) was theoretically calculated by McMichael *et al.*⁸ At sufficiently small applied fields, the crossover length scale is on the order of hundreds of micrometers, which is easily accessible by conventional optical methods.

II. EXPERIMENT

We performed measurements with two techniques to investigate the nature of the linewidth broadening: (1) a spatially integrated ($220\ \mu\text{m}$ by $1\ \text{cm}$) technique of pulsed in-

ductive microwave magnetometry (PIMM) (Ref. 9) which measures the magnetic susceptibility inductively,⁹ and (2) magneto-optical microprobe measurements with a spatial resolution of $1\ \mu\text{m}$ to explore the source of line broadening, which is inferred from the spatially integrated technique. With the spatially resolved technique we are able to probe local variations in the resonance frequency at a number of different spatial positions. We find that the spatial variations of the local resonance frequency agree with those predicted by the zero frequency intercept of the PIMM linewidth data.

The sample used in this study was a $1\ \text{cm} \times 1\ \text{cm} \times 10\ \text{nm}$ $\text{Ni}_{80}\text{Fe}_{20}$ film grown on a $150\ \mu\text{m}$ glass substrate via dc magnetron sputtering in a dc applied magnetic field to induce a uniaxial anisotropy axis.¹⁰ The coercivity was $120 \pm 40\ \text{A/m}$ and the induced anisotropy was $420 \pm 40\ \text{A/m}$ as determined with a quasistatic inductive magnetometer. The easy axis of the sample was aligned parallel to the center conductor in all measurements. The setup of the PIMM measurement technique is similar to that which was previously reported and used a $220\ \mu\text{m}$ coplanar waveguide.^{9,11} In conjunction with PIMM, we use a time-resolved magneto-optic Kerr effect (TR-MOKE) microprobe for local detection of the magnetization dynamics. The TR-MOKE technique is setup to measure the change in the out-of-plane component of the magnetization. The waveguide excitation source and dc field sources are identical to those used for the PIMM; the only difference lies in the microscopic optical detection rather than the inductive detection of the PIMM. The TR-MOKE microprobe uses the polar geometry with the laser beam incident normal to the sample surface. We use a fast ($50\ \text{ps}$ rise time, $10\ \text{ns}$ duration) magnetic field pulse to excite the dynamics. The laser pulse width was $20\ \text{ps}$. When all of the sources of timing jitter were taken into account, our optical time resolution with the TR-MOKE was better than $50\ \text{ps}$.

Figure 1 shows the time domain signal from both the PIMM and the TR-MOKE, and their corresponding fast Fourier transforms (FFT). The data were taken with an applied bias field of $400\ \text{A/m}$ ($5\ \text{Oe}$) and show the agreement be-

^{a)}Electronic mail: mlschnei@boulder.nist.gov

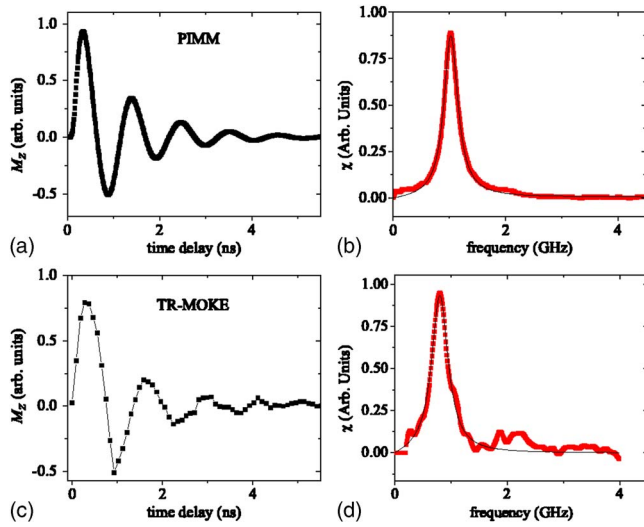


FIG. 1. (Color online) (a) Raw PIMM data taken at $H_b = 400$ A/m (5 Oe) showing the inductive pickup amplitude versus time delay. (b) FFT of the PIMM data in (a). (c) Raw TR-MOKE data taken at 400 A/m (5 Oe) showing the polar optical signal amplitude versus time delay. (d) FFT of the TR-MOKE data in (c).

tween the two measurements. The inset of Fig. 2(a) shows the orientation of our sample with respect to the applied bias field H_b and pulse field H_p . In order to obtain the resonance frequency we use an FFT with zero padding at the end of the time trace to transform the time-domain data into the frequency domain.¹² Once in the frequency domain, we fit the imaginary part of the susceptibility to a harmonic oscillator response function (described in greater detail below).^{9,13,14} Figure 2(a) shows a plot of resonance frequency squared f_0^2 versus applied bias field H_b obtained with the PIMM measurements. We find that f_0^2 is a linear function of H_b , as expected when $H_b \ll M_s$. Data from the TR-MOKE were not included because there were stray fields on the order of 100 A/m created by ferrous components in the objective lens. The effective bias field for the TR-MOKE could be determined from the PIMM data. However, all the analysis presented here was performed with respect to the resonance frequency and therefore required no correction for the stray fields. Nevertheless, f_0^2 for the TR-MOKE data was also a linear function of H_b .

Figure 2(b) shows the effective field-swept linewidth ΔH versus resonance frequency f_0 . We calculate ΔH in the following manner. First, we fit the FFT of the PIMM data to

$$\chi(f) = \frac{\chi_0 f_0^2}{f_0^2 - f^2 - i f \Delta f}, \quad (1)$$

where χ_0 is the dc susceptibility and Δf is approximately equal to the full width at half maximum (FWHM) frequency linewidth in the limit of $f_0 \gg \Delta f$. We then convert to ΔH using¹³

$$\Delta H = \frac{2f_0 \cdot \Delta f}{\left(\frac{\gamma \cdot \mu_0}{2\pi}\right)^2 M_s}, \quad (2)$$

where γ is the gyromagnetic ratio, μ_0 is the permeability of free space, and M_s is the saturation magnetization. The open

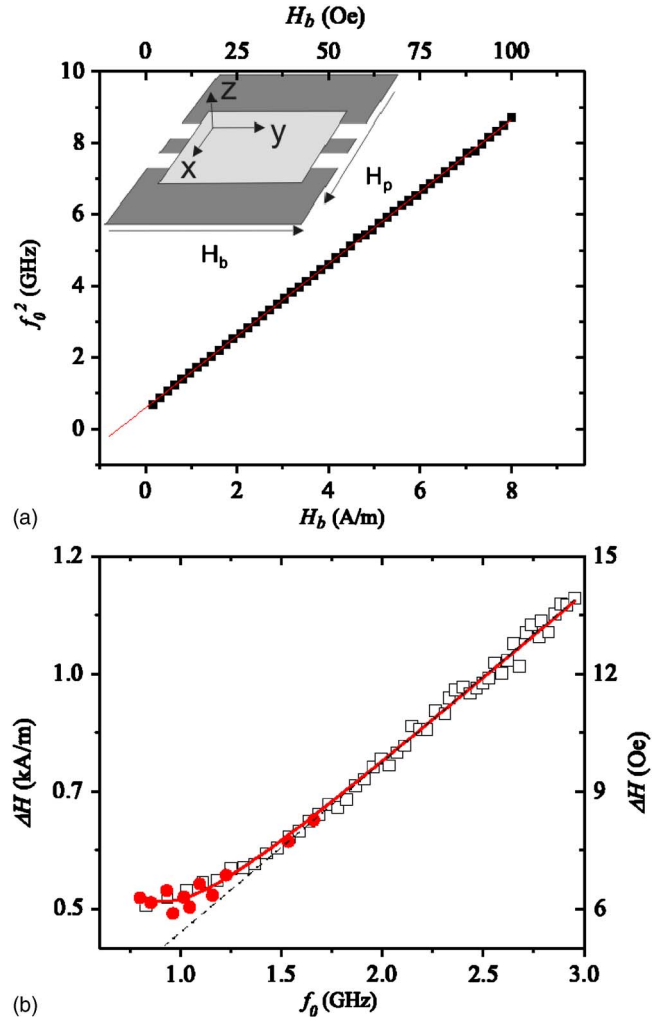


FIG. 2. (Color online) (a) PIMM data of the resonance frequency squared versus the applied field. Inset shows the geometrical layout of the experiment and the applied fields. (b) Calculated field-swept linewidth from the PIMM (open squares) and the TR-MOKE (open circles) as a function of resonance frequency. Linear fit to PIMM data above 1.5 GHz is dashed line, fit to Eq. (4) for all of the PIMM data is shown with the solid line.

squares are data from the PIMM and the open circles are data taken with the TR-MOKE. The limited signal-to-noise ratio of the TR-MOKE precluded our ability to accurately measure the resonance frequency for $H_b > 2.4$ kA/m (30 Oe). The PIMM data for ΔH above 1.5 GHz are nominally linear with frequency and thus lend themselves to traditional slope-intercept analysis as shown in the figure with the dashed line;¹³ data below 1.5 GHz are addressed at the end of this article. Using the data above 1.5 GHz and fitting to a line, we predict a zero-frequency intercept of 88 ± 16 A/m (1.1 ± 0.2 Oe). Because of the limited data from the TR-MOKE above 1.5 GHz we do not apply this same analysis technique to the TR-MOKE data.

The TR-MOKE is used to measure the additional effective line broadening due to localized inhomogeneities, which manifest as variations in the local anisotropy field. As discussed in Ref. 8, the broadening of FMR linewidth via inhomogeneities in thin film samples can be divided into two general regimes: Collective two-magnon scattering and localized inhomogeneous dynamics. If the inhomogeneity

length scale is greater than the critical length scale between collective two-magnon behavior and localized field distributions ($D_K > D_{K,c}$), then the spatial distribution of resonance frequencies correlates with the spatial distribution of anisotropy, and the additional contribution to the FWHM linewidth is approximately $\Delta H_0 = 2\delta H$, where ΔH_0 is the inhomogeneous contribution to the line broadening and δH is the standard deviation of the localized anisotropy fields. If however, $D_K < D_{K,c}$, then the spatial variation of the resonance frequency variation is on the order of $D_{K,c}$, and the additional contribution to the linewidth is a decreasing function of decreasing D_K . Theory and numerical simulations to determine the critical size of the inhomogeneities (i.e., grain size in polycrystalline thin films with random crystalline anisotropy) have previously been reported.⁸ The crossover point at which the behavior changes from collective two magnon to localized field distributions is given by

$$\frac{2(2H + M_s)\delta H}{M_s^2 d} D_{K,c} \approx 2\pi. \quad (3)$$

Here, H is the applied field, M_s is the saturation magnetization, and d is the film thickness. In the limit of localized inhomogeneous broadening, the spatially averaged data taken with the PIMM (above 1.5 GHz) predicts that $\Delta H_0 = 88$ A/m (1.1 Oe), meaning that one would expect a local field standard deviation $\delta H = 44$ A/m (0.55 Oe). In this case $D_{K,c} = 550$ μm at $H_b = 80$ A/m and 10 nm film thickness. In the case of collective two-magnon scattering where $D_{K,c} < 550$ μm , one would expect that $\delta H > 44$ A/m.

Figure 3(a) shows the resonance frequency measured with the TR-MOKE as a function of the position of the optical spot on the sample scanned down the length of the coplanar waveguide (CPW) line along the y axis, with measurements spaced 500 μm apart over a total measurement distance of 5 mm. Data are shown for several fields, and, as was expected, there is no clear trend with the position along the length of the center conductor. We interpret the variation in the spatial frequency as a function of position as the result of localized variations of the effective field, perhaps as a result of spatial variations in the anisotropy energy density. One expects a strong variation of the resonance frequency if the scan were to be taken across the width of the CPW line. This is a result of magnetostatic surface waves and has been well described previously.^{6,7}

Figure 3(b) shows the corresponding field fluctuation δH that was measured as the standard deviation of the resonance frequency about the average resonance frequency $\langle f_0 \rangle$ obtained for a given value of applied field. This number was determined from Eq. (2), where δf was used to calculate the value of δH . There appears to be no functional dependence of δH on resonance frequency in the data range that we measured. We therefore averaged all of the values together and determined the root mean square field fluctuation value is $\delta H = 40 \pm 4$ A/m (0.50 \pm 0.05 Oe), which agrees well with the predicted value from the PIMM linewidth measurements. We conclude that the slope-intercept method for extracting the inhomogeneous contribution to the linewidth from PIMM data is an accurate means of determining the spatial variation of resonance frequency in Permalloy films.

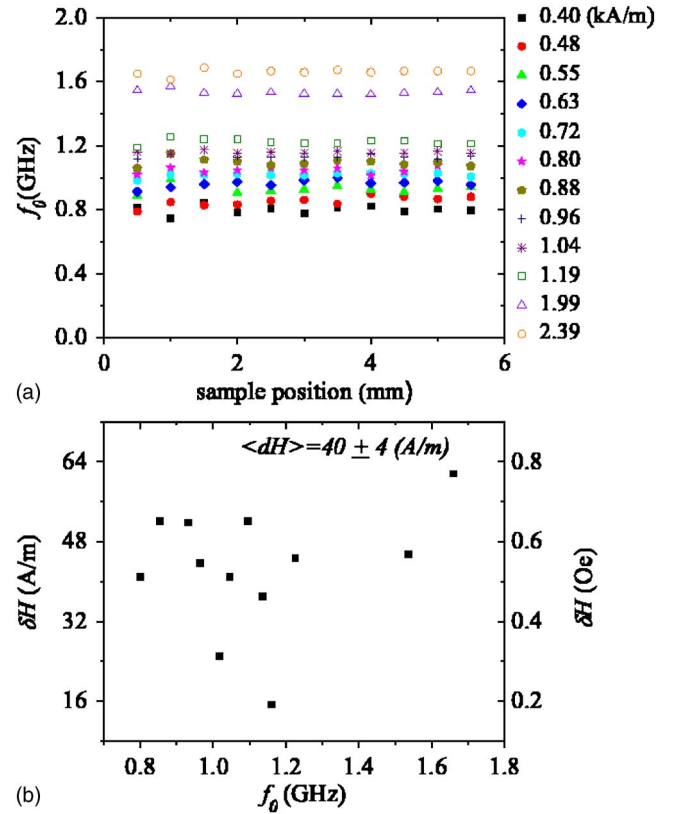


FIG. 3. (Color online) (a) TR-MOKE data for resonance frequency versus sample position for several values of H_b . Error bars are equal to the size of the data points. (b) Calculated linewidth broadening as a result of the variation of the resonance frequency with position for a given mean resonance frequency. The average value of the broadening for all resonance frequencies is given by $\langle \delta H \rangle$.

III. DISCUSSION

It was previously found that linewidth data for various thin film NiFe alloys are well fit by inclusion of an additional power law term in the fitting function.¹⁵ Figure 2(b) shows a fit to all of the data when an additional power-law term is added to the fitting with a solid line. The fitting function now includes three terms and has the following form:

$$\Delta H = \Delta H_0 + \frac{4\pi\alpha}{\gamma\mu_0} f + \left(\frac{\eta_0}{f} \right)^\beta, \quad (4)$$

where η_0 is a proportionality constant and β is the frequency exponent. Inclusion of a power law term in the fitting function greatly improves the quality of the fit, especially at frequencies below 1.5 GHz. We obtain fitting values of $\beta = 3.3 \pm 0.5$ with $\alpha = 0.006$ and $\eta_0 = 5.2 \times 10^2$ Hz (A/m) $^{-\beta}$. We locked ΔH_0 to 80 A/m (1 Oe), which is our best estimate of the value from spatially resolved TR-MOKE measurements. If we allow ΔH_0 to be a fitting variable, it tends toward zero and does not appreciably alter the fit, but does result in a value of $\beta = 1.9$.

The observed power-law behavior does not agree with the predictions of classical Hoffman ripple theory, where dispersion of the internal dipole fields associated with the ripple pattern can be a source of line broadening.¹⁶ In the case of the classical theory for ripple-induced resonance frequency dispersion, the field-swept linewidth indeed has a power law

component, but the exponent is $\beta=1/2$. It is clear from our measurements that enhanced linewidth at low frequencies is not simply the result of the nonuniform magnetization distribution alone.

We speculate that one possible explanation for the additional term is the existence of dynamically driven magnetic instabilities, or magnetic “flicker” noise,^{17–20} though we do not find a quantitative reason for $\beta=3.3$ due to the magnetic flicker noise. If one includes the crystalline energy of the individual grains in a polycrystalline film and assumes that the exchange energy acts to average the variations in anisotropy energy, the magnetization will have a nonuniform distribution,²¹ i.e., magnetic ripple. Given the large number of spatial degrees of freedom that are presumed to give rise to magnetic ripple, it is reasonable to assume that there is also a multiplicity of different, though nearly degenerate, ripple distributions that the magnetization could exhibit. It is well known that thermal fluctuations can drive the magnetization between different metastable degenerate configurations,²² as was recently observed by Lorentz-mode transmission electron microscopy TEM in thin films at length scales as short as 200 nm.²⁰ Furthermore, we expect from the fluctuation-dissipation theorem that the thermal fluctuations should be manifested as increased damping at low frequencies.²³ We therefore speculate that magnetic ripple may present an additional source of line broadening thin film systems when measured at low frequencies.

From our linewidth versus frequency data, the magnetic noise in the system does not follow a $1/f$ scaling. For example, spin waves and phonons have very different dispersion behavior, precluding typical thermal phonon dependence for magnetic fluctuations. However, in the absence of any theoretical treatment of the dynamic spectrum for ripple instabilities in an ac applied field, theoretical predictions do not yet exist against which we can compare our experimentally determined exponent β .

IV. CONCLUSION

In conclusion, a previous theory establishes a minimum critical spacing between magnetic inhomogeneities for linewidth broadening to be considered localized in character.⁸ When optically probing at smaller than the critical length

scale, we are able to establish an upper bound of localized field variation of $\Delta H_0=80$ A/m (1 Oe). This agrees well with what is found from linewidth versus frequency PIMM data. By using the two separate techniques we are able to determine the value of ΔH_0 in the fitting but we still require an additional power law term in order to adequately fit the data below 1.5 GHz. The power law dependence is not of the correct exponent for simple ripple effects from classical Hoffman ripple theory. We speculate that this increase may be due to magnetic noise from random hopping between multiple ground state configurations.

¹Z. Celinski and B. Heinrich, J. Appl. Phys. **70**, 5935 (1991).

²F. J. Cadieu, R. Rani, W. Mendoza, B. Peng, S. A. Shaheen, M. J. Hurben, and C. E. Patton, J. Appl. Phys. **81**, 4801 (1997).

³M. Covington, T. M. Crawford, and G. J. Parker, Phys. Rev. Lett. **89**, 237202 (2002).

⁴S. G. Reidy, L. Cheng, and W. E. Bailey, Appl. Phys. Lett. **82**, 1254 (2003).

⁵A. Barman, V. V. Kruglyak, R. J. Hicken, A. Kundrotaitė, and M. Rahman, Appl. Phys. Lett. **82**, 3065 (2003).

⁶G. Counil, J.-V. Kim, T. Devolder, C. Chappert, K. Shigeto, and Y. Otani, J. Appl. Phys. **95**, 5646 (2004).

⁷M. L. Schneider, T. Gerrits, A. B. Kos, and T. J. Silva, Appl. Phys. Lett. **87**, 072509 (2005).

⁸R. D. McMichael, D. J. Twisselmann, and A. Kunz, Phys. Rev. Lett. **90**, 227601 (2003).

⁹T. J. Silva, C. S. Lee, T. M. Crawford, and C. T. Rogers, J. Appl. Phys. **85**, 7849 (1999).

¹⁰M. L. Schneider, A. B. Kos, and T. J. Silva, Appl. Phys. Lett. **85**, 254 (2004).

¹¹A. B. Kos, T. J. Silva, and P. Kabos, Rev. Sci. Instrum. **73**, 3563 (2002).

¹²C. D. McGillem and G. R. Cooper, *Continuous and Discrete Signal and System Analysis* (Holt, Rinehart, Winston, New York, 1984), p. 180.

¹³S. S. Kalarickal, P. Krivosik, M. Z. Wu, C. E. Patton, M. L. Schneider, P. Kabos, T. J. Silva, and J. P. Nibarger, J. Appl. Phys. **99**, 093909 (2006).

¹⁴C. Alexander, J. Rantschler, T. J. Silva, and P. Kabos, J. Appl. Phys. **87**, 6633 (2000).

¹⁵R. Bonin, M. L. Schneider, T. J. Silva, and J. P. Nibarger, J. Appl. Phys. **98**, 123904 (2005).

¹⁶J. O. Rantschler and C. Alexander, Jr., J. Appl. Phys. **93**, 6665 (2003).

¹⁷N. Giordano, Phys. Rev. B **53**, 14937 (1996).

¹⁸C. D. Keener and M. B. Weissman, Phys. Rev. B **49**, 3944 (1994).

¹⁹P. Dutta and P. M. Horn, Rev. Mod. Phys. **53**, 497 (1981).

²⁰J. M. Shaw, R. Geiss, and S. E. Russek, Appl. Phys. Lett. **89**, 212503 (2006).

²¹H. Hoffmann, IEEE Trans. Magn. **4**, 32 (1968).

²²P. Kabos, S. Kaka, S. E. Russek, and T. J. Silva, IEEE Trans. Magn. **36**, 3050 (2000).

²³N. Smith and P. Arnett, Appl. Phys. Lett. **78**, 1448 (2001).